Resolution of a possible misinterpretation of the nuclear excitation mode along the yrast line: An investigation on the evolution of rotation and vibration

Hai-Yan Meng and Hua-Lei Wang *
School of Physics and Microelectronics, Zhengzhou University, Zhengzhou 450001, China

Min-Liang Liu
Key Laboratory of High Precision Nuclear Spectroscopy, Institute of Modern Physics, Chinese Academy of Sciences, Lanzhou 730000, China and School of Nuclear Science and Technology, University of Chinese Academy of Sciences, Beijing 100049, China

(Received 8 October 2021; accepted 24 December 2021; published 20 January 2022)

An empirical approach, called E-GOS (E-gamma over spin) curves, which is used for discerning the evolution between vibration and rotation in nuclei as a function of spin, is discussed. Considering the possible mechanisms and the results of total-Routhian-surface calculations, we find that the decrease in an E-GOS plot may be misinterpreted as the onset of vibration behavior along the yrast line. The insufficiency of the vibration-like criterion of the E-GOS curves to determine the transition from rotation to vibration is emphasized. It is pointed out that the crossing between the ground-state and S bands, especially with a strong interaction, will be responsible for such vibration-like evolution of nuclear excitation modes.

DOI: 10.1103/PhysRevC.105.014315

I. INTRODUCTION

Atomic nuclei are composed of interacting nucleons (fermions) but there is increasing evidence that collective excitations resulting in both vibrations and rotations occur. Moreover, it has been found that the collective excitation modes can evolve with respect to different nuclear degrees of freedom, such as nucleon number, excitation energy, and angular momentum [1]. Generally speaking, such an evolution is intimately related to shape/phase transition, which is one of the most significant topics in nuclear structure research [2]. For instance, it was pointed out that shape or phase transition from vibration to axial rotation or γ-unstable rotation, or even a triple point, may appear with the variation of neutron number [1,3,4]. One is also interested in the state evolution along the yrast line since the yrast states are usually favorable to be populated in experiments, especially via the heavy-ion fusion-evaporation reaction. Note that the yrast line is formed by the cascades of all yrast states—the lowest energy state for a given I. Indeed, some interesting phenomena such as the band crossing (back-bending effect), yrast traps, and shape transitions were identified and discussed along the yrast line where various excitation modes may compete and/or couple in different ways [5,6]. As is known, even in one motion mode, there may be involved different collective characteristics (e.g., with different configurations) along the yrast line [7].

In 2003, Regan *et al.* [8] proposed a new empirical way, the ratio $R(I)$ [$\equiv E_\gamma(I \to I-2)/I$] versus angular momentum I [the so-called E-GOS (E-gamma over spin) curve], to determine the vibrational-to-rotational evolution along the yrast line. For a perfectly harmonic quantum vibrator and axially symmetric rotor, the energy sequence can be given respectively by $E_I = n\hbar\omega$ [9] and $E_I = [\hbar^2/(2J)]I(I+1)$ [10], where the phonon number $n = I/2$ and J is the static moment of inertia. Correspondingly, the function relationships between $R(I)$ and I are easily derived to be $\frac{\hbar\omega}{I}$ and $\frac{\hbar^2}{2J}(4-\frac{2}{I})$ for the above vibrator and rotor, respectively. In the $A \approx 100$ mass region, some nuclei clearly exhibit transitions from vibration to rotation along the yrast line [8]. Soon after, Liu *et al.* [2] proposed a model associated with the U(5) symmetry in the interacting boson model (IBM) to describe the rotation driven vibrational to axially rotational shape phase transition along the yrast line.

Naturally, one expects to see whether the opposite evolution, from rotation to vibration, can occur with the help of such an empirical approach. From the decreasing trends of the E-GOS curves, it seems that such opposite patterns appear in some nuclei; see, e.g., Refs. [11–15]. It should be noted that this reducing behavior is very likely to be misinterpreted and rather necessary to be clarified though the improved centipede-like E-GOS curves given in our previous publications [12–15]; where we tried to consider the possible variation of the vibrating frequency and moment of inertia, and even the first-order vibration-rotation coupling. One should pay attention to not only the function relationship but also the first and second derivatives of the E-GOS curve. Even so, it may be still not enough to determine the evolution from rotation to vibration by this empirical way. In this paper, we will focus on the possible evolution between rotation and vibration, discussing the necessary and/or sufficient condition(s) of the shape/phrase transitions based on the total-Routhian-surface (TRS) calculation [16–19].

*wanghualei@zzu.edu.cn

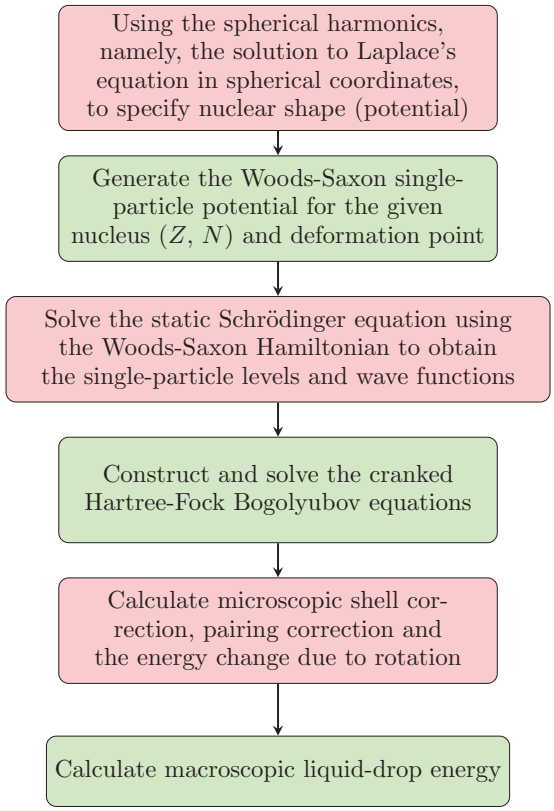

FIG. 1. The general procedure of TRS calculation.

We organize the present project as follows. In Sec. II, we give a brief description of the TRS method, together with the necessary references. The results and discussion are presented in Sec. III. A summary is given in Sec. IV.

II. TOTAL-ROUTHIAN-SURFACE METHOD

We will give a short presentation of the unified procedure of the TRS method below, including the necessary references. The TRS calculation, combined with the realistic Woods-Saxon potential, is powerful and widely used in nuclear structure research [17–19]. This theoretical treatment is based on the macroscopic-microscopic model [20,21] and the one-dimensional cranking approximation [22–24]. The usual expression for the total energy of the rotating nuclear system (namely, the so-called total Routhian) reads (see, e.g., Refs. [25,26],

$$\begin{aligned} E^{\omega}(Z,N,\hat{\beta}) &= E_{LD}(Z,N,\hat{\beta}) \\ &+ \delta E_{\text{shell}}(Z,N,\hat{\beta}) + \delta E_{\text{pair}}(Z,N,\hat{\beta}) \\ &+ [\langle \hat{H}^{\omega}(Z,N,\hat{\beta})\rangle - \langle \hat{H}^{\omega=0}(Z,N,\hat{\beta})\rangle]. \end{aligned} \quad (1)$$

Generally, we can carry out the calculation in six standard steps, as seen in Fig. 1. Then, one can obtain the total Routhian by the sum of macroscopic and microscopic energies obtained in the last two steps.

In this work, we calculate the deformed Woods-Saxon (WS) potential at each $(\beta_2, \gamma, \beta_4)$ deformation lattice. The basis of the axially deformed harmonic oscillator in the cylindrical coordinate system is used to generate the Hamiltonian matrix. Then the single-particle levels and wave functions are obtained by diagonalizing the Hamiltonian matrix. The shell and pairing corrections are respectively calculated by using the Strutinsky method [27] and the Lipkin-Nogami (LN) method [28]. This LN method can avoid the spurious pairing phase transition occurring in the traditional Bardeen-Cooper-Schrieffer (BCS) treatment. Moreover, besides monopole pairing, doubly stretched quadrupole pairings are considered, which will be important for the proper description of, e.g., nuclear moment of inertia and back-bending frequency, though they have a negligible effect on energy [29]. The monopole pairing strength, G, is estimated by the average gap method [30] and the quadrupole pairing strengths are calculated by restoring the Galilean invariance broken by the seniority pairing force [31,32]. The adopted pairing windows for both protons and neutrons contain dozens of single-particle levels, e.g., half of the particle number Z and N, below and above the Fermi surface. Under rotation, it is supposed that nuclear system with a fixed shape is cranked around a principal axis [33]. Equivalently, only one Euler angle changes without the inclusion of nuclear vibration, which corresponds to the variation of the collective coordinates around their equilibrium positions. The resulting cranking LN equation takes the form of the well known Hartree-Fock-Bogolyubov-like (HFB) equation which can be solved by using the HFB cranking (HFBC) method [6,34]. While solving the HFBC equations, pairing is treated self-consistently at each frequency ω and each grid point in the selected deformation space. The macroscopic energy is calculated by the standard liquid drop (LD) model with the original model parameters [35].

At the end, the total Routhian of a rotating nucleus can be calculated according to the procedure described above at each deformation grid. The smoothed TRS will be obtained by interpolating between the calculated sampling points. The nuclear properties including the equilibrium deformations can be extracted from the minimum of the TRS and other physical quantities, e.g., aligned angular momenta, can be analyzed at the equilibrium state.

III. RESULTS AND DISCUSSION

Based on the idealized assumption of collective excitations, we can give some empirical plots as seen below. Figure 2(a) shows the empirical E-GOS curve for a perfect harmonic vibrator and axially symmetric rotor with the first 2^+ excitations of 500 and 100 keV, respectively (same as Fig. 2(a) in Ref. [8]). The inset in Fig. 2(a) give the corresponding moment of inertia, J ($\equiv I_x/\omega$). One can notice that the moment of inertia J and rotational frequency ω keep the constant numbers 30 $\hbar^2\text{MeV}^{-1}$ and $0.25\hbar\omega$ for the ideal rotor and vibrator, respectively, in the J-ω plot. Figure 2(b) shows the schematic diagrams of the energy sequences $E(I)$ for two ideal vibrators and two rotors. For the ground-state bands, these lines and curves, respectively, corresponding to vibrators and rotors, will cross the origin of the coordinates. The inset (b1) in Fig. 2(b) shows the rotation driven vibrational to axially rotational phase transition along the yrast

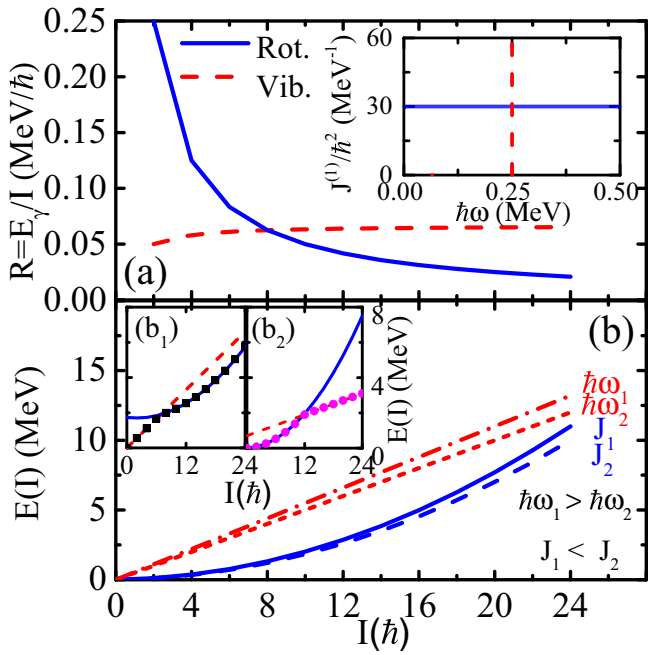

FIG. 2. (a) Typical E-GOS curves for a perfect harmonic vibrator (red dashed line) and axially symmetric rotor (blue solid line), respectively. The inset in (a) denotes the moment of inertia for them, see the text for more details. (b) The energies against spin I for two ideal vibrators ($\hbar\omega_2 = 1.1\hbar\omega_1$) and rotors ($J_2 = 1.1J_1$). Two insets (b1) and (b2) indicate the phase transitions from vibration to rotation and from rotation to vibration, respectively.

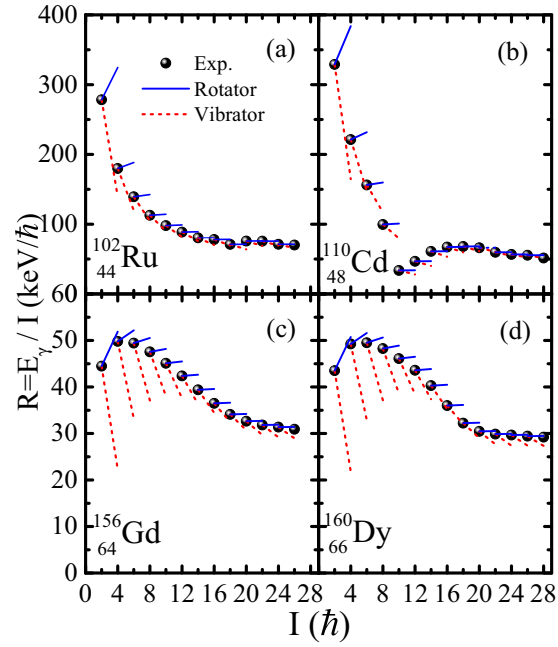

FIG. 3. The centipede-like E-GOS curves along the yrast sequences for even-even nuclei ^{102}Ru (a), ^{110}Cd (b), ^{156}Gd (c), and ^{160}Dy (d).

line, similar to Fig. 3 in Ref. [2]. In contrast, the inset (b2) in Fig. 2(b) is expected to describe the rotational to vibrational phase transition but the experimental evidence is not sufficient so far.

In the present investigation, we will focus on two groups of even-even nuclei which have different evolution properties along the yrast line. Note that all the candidate nuclei are taken from the previous publications [2,8,11–15]. In Table I, we list the nuclei with the evolution signature from vibration to rotation along the yrast line. In contrast, the nuclei listed in Table II are suggested to have the opposite evolution signature (from rotation to vibration) based on the emperical E-GOS curve.

In order to evaluate the ground-state properties of these candidate nuclei and check the calculated results with two sets of Woods-Saxon parameters, we show the phenomenological $R_{4/2}$ ratio, P factor, and experimental and theoretical β_2 deformations. The energy ratio of the first 4_1^+ and 2_1^+ excited states in even-even nuclei, namely, $R_{4/2}$ [$\equiv E(4_1^+)/E(2_1^+)$], is generally regarded as a good indicator of different collective motions and critical point symmetries of a nucleus, especially in low-lying nuclear structure (e.g., see Ref. [13] and references therein for more details, where nine frequently used critical points are given and discussed). Besides the $R_{4/2}$ ratio, another more sensitive phenomenological quantity related to nuclear collectivity and deformation is the P factor [40–44]. We point out that when each valence nucleon generally interacts with about 4–5 nucleons of the other type, namely, $P \approx 4$–5, the transition to deformation will take place. Indeed, one can see that, in Table I, the nuclei with expected vibrating properties at ground states have smaller $R_{4/2}$ and P values; whereas the nuclei with relatively large $R_{4/2}$ and P values in Table II indicate large collectivities. Two sets of WS parameters can give similar results which slightly underestimate the experimental β_2 values, agreeing with the systematic analysis by Dudek *et al.* [45]. The experimental β_2 obtained from $B(E2)$ automatically includes the vibrating effect while the value from Q does not. As expected, the available data show that the experimental β_2 values obtained from $B(E2)$ are systematically bigger than those from Q values, as seen in Table I, in good agreement with the vibration mode at low spins. Two experimental β_2 values of those nuclei in Table II possess the same order of magnitude but several ones with opposite sign are desired to be studied in the future. To some extent, the difference between these two kinds of β_2 values may be regarded as an empirical indicator of the existence of dynamic deformations. Considering the evolution mode and one type of measured β_2 values, one may evaluate the other types of measurements [e.g., the $B(E2)$ or Q values].

Taking as examples four previously published even-even nuclei, ^{102}Ru, ^{110}Cd, ^{156}Gd, and ^{160}Dy [8,11], Fig. 3 shows the centipede-like E-GOS curves (e.g., cf. Refs. [12–14]). It was reported that the nuclei ^{102}Ru and ^{110}Cd evolve from vibration to rotation [8]. However, in Ref. [11], it was pointed out that ^{156}Gd and ^{160}Dy exhibit the signature from rotation to vibration along the yrast line based on the evolution trend of the E-GOS curve. Indeed, this assignment is somewhat risky since the decrease of the E-GOS curve is not a sufficient condition of the occurrence of rotation to vibration. For instance, as

TABLE I. The extracted $R_{4/2}$ ratios, P factors and the calculated (Uni.: with universal parameter set [36]; Cra.: with cranking parameters [37]) and available experimental (Expt. 1: from $B(E2)$ [38]; Expt. 2: from Q [39]) deformation parameter β_2 for nuclei which have the evolution signature from vibration to rotation along the yrast line [8,12–14].

Nuclei	$R_{4/2}$	P	β_2			
			Uni.	Cra.	Expt. 1	Expt .2[a]
^{98}Mo	1.92	3.43	0.20[21][b]	0.20[27]	0.17	0.09
^{100}Mo	2.12	4.00	0.24[9]	0.24[21]	0.23	0.10
^{102}Mo	2.51	4.44	0.29	0.28[19]	0.31	
^{104}Mo	2.92	4.80	0.31[15]	0.32[17]	0.36	
^{106}Mo	3.04	5.09	0.32[18]	0.32[19]	0.35	
^{108}Mo	2.92	5.33	0.32	0.33	0.38	
^{100}Ru	2.27	3.00	0.16	0.17	0.21	0.12
^{102}Ru	2.33	3.43	0.21[19]	0.21[18]	0.24	0.17
^{104}Ru	2.48	3.75	0.24[25]	0.25[24]	0.27	0.18
^{106}Ru	2.65	4.00	0.26[24]	0.27[23]	0.26	
^{108}Ru	2.75	4.20	0.28[24]	0.28[22]	0.29	
^{110}Ru	2.76	4.36	0.28[25]	0.29[27]	0.29	
^{102}Pd	2.29	2.40	0.14	0.16	0.20	0.06
^{104}Pd	2.38	2.67	0.17	0.17	0.21	0.14
^{106}Pd	2.40	2.86	0.18	0.17	0.23	0.15
^{108}Pd	2.42	3.00	0.21[21]	0.21[16]	0.24	0.17
^{110}Pd	2.46	3.11	0.22[22]	0.24[21]	0.26	0.14
^{112}Pd	2.53	3.20	0.23[51]	0.24[40]	0.22	
^{104}Cd	2.27	1.50	0.11	0.13	0.17	
^{106}Cd	2.36	1.60	0.13	0.14	0.17	0.08
^{108}Cd	2.38	1.67	0.13	0.14	0.18	0.13
^{110}Cd	2.23	1.71	0.14	0.14	0.18	0.11
^{112}Cd	2.29	1.75	0.14	0.14	0.19	0.11
^{114}Cd	2.40	1.78	0.15	0.15	0.19	0.11
^{118}Ba	2.86	4.00	0.29	0.29		
^{120}Ba	2.92	4.20	0.28[7]	0.28[10]		
^{122}Ba	2.90	4.36	0.26	0.27	0.35	
^{124}Ba	2.83	4.20	0.25	0.26	0.30	
^{126}Ba	2.78	4.00	0.24	0.25	0.27	
^{128}Ba	2.69	3.75	0.21	0.21	0.25	
^{156}Hf	1.85	1.67	0.06	0.08		
^{158}Hf	2.17	2.86	0.12	0.13		
^{160}Hf	2.30	3.75	0.15	0.16		
^{162}Hf	2.56	4.44	0.18	0.18	0.16	
^{164}Hf	2.79	5.00	0.20	0.20	0.20	
^{166}Hf	2.97	5.45	0.22	0.22	0.25	
^{160}W	2.07	2.67	0.11	0.12		
^{162}W	2.25	3.43	0.14	0.15		
^{164}W	2.48	4.00	0.16	0.17		
^{166}W	2.68	4.44	0.18	0.18		
^{168}W	2.82	4.80	0.20	0.20	0.23	
^{170}W	2.95	5.09	0.21	0.21	0.24	

[a]The average β_2 is adopted if there are several measured Q values.
[b]The value in the square brackets denotes the calculated γ which is given if it is greater than 5°.

shown in Figs. 3(c) or 3(d), one can see that the decrease of the E-GOS curve can be reproduced by the variation of moment of inertia. As can be seen from Fig. 2, the vibrating behavior exhibits a constant ω value. In the up-bending or back-bending region, the vibration-like behavior may appear, indicating that the band crossing may be responsible for the deduced E-GOS curve.

TABLE II. Same as Table I but for nuclei with the opposite signature (e.g., evoluving from rotation to vibration) [11,12,14,15].

Nuclei	$R_{4/2}$	P	β_2			
			Uni.	Cra.	Expt. 1	Expt. 2
^{156}Gd	3.24	5.83	0.26	0.26	0.34	0.34
^{158}Gd	3.29	6.46	0.27	0.27	0.35	0.34
^{160}Gd	3.30	7.00	0.28	0.28	0.35	0.35
^{162}Gd	3.30	7.47	0.28	0.29		
^{158}Dy	3.21	5.83	0.25	0.26	0.33	
^{160}Dy	3.27	6.86	0.27	0.27	0.34	−0.30
^{162}Dy	3.29	7.47	0.28	0.28	0.34	
^{164}Dy	3.30	8.00	0.28	0.29	0.35	0.34
^{170}Yb	3.29	7.20	0.29	0.29	0.33	−0.31
^{172}Yb	3.30	7.50	0.29	0.29	0.33	
^{174}Yb	3.30	7.76	0.28	0.29	0.32	−0.31
^{176}Yb	3.31	7.50	0.28	0.28	0.30	−0.32
^{174}Hf	3.27	6.67	0.28	0.29	0.29	
^{176}Hf	3.29	6.88	0.27	0.27	0.30	0.30
^{178}Hf	3.29	6.67	0.26	0.26	0.28	0.28
^{180}Hf	3.31	6.43	0.26	0.26	0.27	0.28
^{180}W	3.26	5.71	0.23	0.24	0.25	−0.28
^{182}W	3.29	5.54	0.23	0.23	0.25	0.28
^{184}W	3.27	5.33	0.22	0.22	0.24	0.25
^{186}W	3.23	5.09	0.20	0.21	0.23	0.21
^{236}Pu	3.30	6.86	0.21	0.22		
^{238}Pu	3.31	7.20	0.22	0.22	0.29	
^{240}Pu	3.31	7.50	0.23	0.22	0.29	
^{242}Pu	3.31	7.76	0.23	0.23	0.29	

To display the possible band crossings, we show, in Fig. 4, the calculated and experimental kinematic moments of inertia of four even-even nuclei as mentioned above. Note that the kinematic moments of inertia are, respectively, calculated by $J^{(1)} = I_x/\omega$ and $J^{(1)} = \hbar^2(2I-1)/E_\gamma(I \to I-2)$ theoretically and experimentally [6]. It can be found that near the band crossing the moment of inertia rapidly increases as the rotational frequency changes slightly, similar to the case in the inset of Fig. 2(a). Since the present TRS calculation does not include the vibrating effect, the disagreement between experiment and theory at low frequency in ^{110}Cd and ^{102}Ru may indicate the appearance of the vibrating behaviors to an extent.

In principle, the onset of the phase transition is related to nuclear shape and its softness. For instance, as described in Ref. [2] (e.g., see Fig. 2 therein), the evolution from vibration to rotation may occur when the shape evolves from spherical or weakly deformed to well-deformed shape. In contrast, to observe the evolution from rotation to vibration, one expects that nuclear deformation, e.g., β_2, will shrink and/or nuclear softness will increase along the yrast line.

We selected ^{102}Ru [8] and ^{156}Gd [11] as example nuclei to investigate their deformation and softness properties, as seen in Figs. 5 and 6, respectively. From Fig. 5, one can see that both nuclei have deformed shapes with relatively

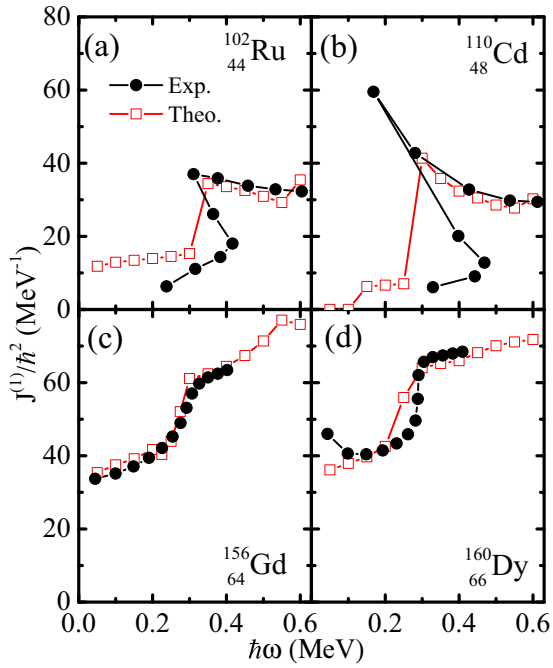

FIG. 4. The experimental and calculated (with cranking parameters) kinematic moments of inertia $J^{(1)}$ for even-even nuclei ^{102}Ru (a), ^{110}Cd (b), ^{156}Gd (c), and ^{160}Dy (d).

large β_2 values. From $\hbar\omega = 0.0$ to 0.6 MeV, the spherical or weakly deformed shape does not appear, not only for ^{102}Ru but also for ^{156}Gd. However, there is a triaxial γ deformation jump near $\hbar\omega = 0.3$ MeV for ^{102}Ru, indicating a possibly large softness in the triaxial direction responsible for the appearance of the vibrating behavior. Indeed, as seen in Fig. 6(a), one can see that the potential energy surface near the minimum is rather flat in the γ direction at low rotational frequency. After the back-bending (cf. Fig. 4), as

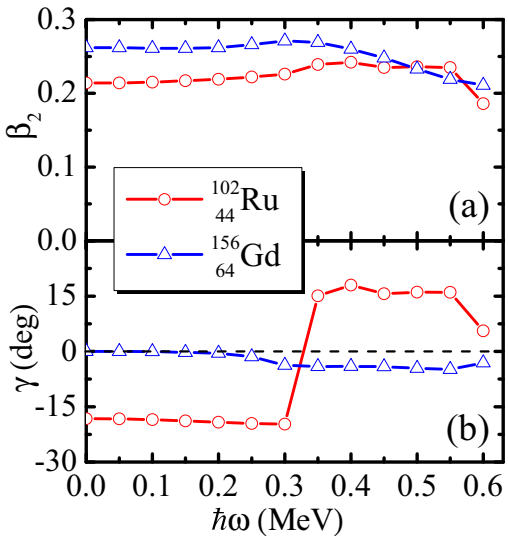

FIG. 5. Calculated β_2 (a) and γ (b) versus $\hbar\omega$ for ^{102}Ru and ^{156}Gd nuclei.

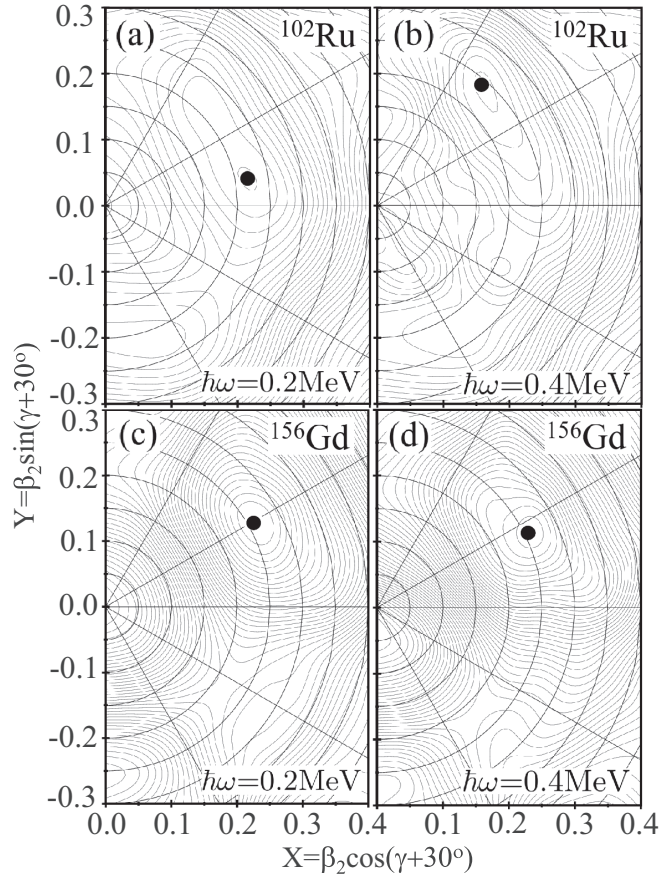

FIG. 6. TRS plots in the (β_2, γ) plane for ^{102}Ru and ^{156}Gd. The black dots indicate the minima and the contour lines are separated by 200 keV.

seen in Fig. 6(b), the minimum becomes stiff, in agreement with the rotational property. It needs to be stressed that neither deformations nor softness can support the possible evolution from rotation to vibration in ^{156}Gd from the present investigation. The vibration-like E-GOS curve should be explained by the variation of moment of inertia and the band crossing.

Figure 7 shows the calculated aligned angular momenta, including the proton and neutron contributions, for the selected nuclei ^{102}Ru and ^{156}Gd. It is seen that the angular momentum alignment of a pair of neutrons is responsible for the band crossing. The slow neutron alignment in ^{156}Gd indicates there is a strong interaction between the ground and S bands. Such a strong interaction will break the $I(I+1)$ rule of both interacting rotational bands, resulting in the small energy difference between two neighboring γ transitions. Therefore, the vibration-like behaviors seem to occur along the yrast line, which may be misinterpreted from the empirical E-GOS curve.

IV. SUMMARY

We discuss the empirical E-GOS curve, which is used for discerning the evolution between vibration and rotation based on the available experimental information and TRS

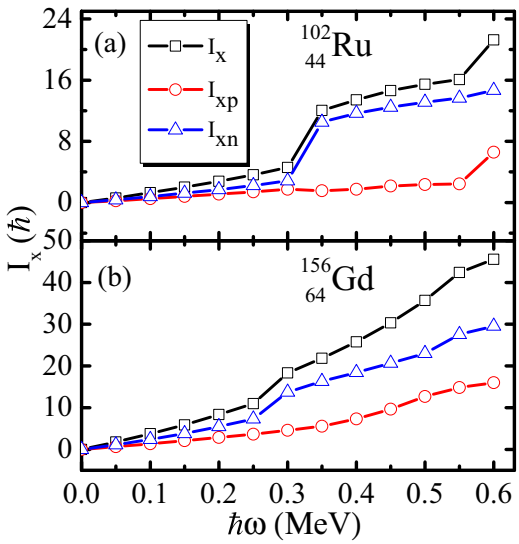

FIG. 7. The calculated aligned angular momenta I_x (squares), including the proton I_{xp} (circles) and neutron I_n (triangles) components, for even-even nuclei ^{102}Ru (a) and ^{156}Gd (b) as a function of the rotational frequency $\hbar\omega$.

calculation. We find that the decrease in an E-GOS plot may be misinterpreted and misused as onset of vibration behavior. The difference between two kinds of experimental β_2 values, e.g., obtained from $B(E2)$ and Q, may be regarded as an empirical indicator of the existence of dynamic deformations. In general, the vibrational-like behavior of the E-GOS curves from rotation to vibration can be attributed to the band crossing and/or the variation of moment of inertia, especially in the well-deformed nuclei. It should be pointed out that the Coriolis force tends to break the pairs and make the moment of inertia increase, and therefore the nuclei will prefer rotational excitations. The evolution from rotation to vibration may theoretically exist but the experimental evidence is not sufficient at present. It may be interesting to search the typical candidates with the evolution properties from rotation to vibration in experiments.

ACKNOWLEDGMENTS

This work was supported by the National Natural Science Foundation of China (No. 11975209, No. U2032211, and No. 12075287), the Physics Research and Development Program of Zhengzhou University (No. 32410017), the Project of Youth Backbone Teachers of Colleges and Universities of Henan Province (No. 2017GGJS008), and the Polish National Science Centre under Contract No. 2016/21/B/ST2/01227. Some of the calculations were conducted at the National Supercomputing Center in Zhengzhou.

[1] F. Iachello and A. Arima, *The Interacting Boson Model* (Cambridge University Press, Cambridge, 1987).
[2] Y. X. Liu, L. Z. Mu, and H. Q. Wei, Approach to the rotation driven vibrational to axially rotational shape phase transition along the yrast line of a nucleus, Phys. Lett. B **633**, 49 (2006).
[3] J. Jolie, P. Cejnar, R. F. Casten, S. Heinze, A. Linnemann, and V. Werner, Triple Point of Nuclear Deformations, Phys. Rev. Lett. **89**, 182502 (2002).
[4] D. Warner, A triple point in nuclei, Nature (London) **420**, 614 (2002).
[5] A. Johnson, H. Ryde, and S. A. Hjorth, Nuclear moment of inertia at high rotational frequencies, Nucl. Phys. A **179**, 753 (1972).
[6] M. J. A. de Voigt, J. Dudek, and Z. Szymanski, High-spin phenomena in atomic nuclei, Rev. Mod. Phys. **55**, 949 (1983).
[7] F. S. Stephens and R. S. Simon, Coriolis effects in the yrast states, Nucl. Phys. A **183**, 257 (1972).
[8] P. H. Regan, C. W. Beausang, N. V. Zamfir, R. F. Casten, J.-y. Zhang, A. D. Yamamoto, M. A. Caprio, G. Grdal, A. A. Hecht, C. Hutter, R. Krcken, S. D. Langdown, D. A. Meyer, and J. J. Ressler, Signature for Vibrational to Rotational Evolution Along the Yrast Line, Phys. Rev. Lett. **90**, 152502 (2003).
[9] G. Scharff-Goldhaber and J. J. Weneser, System of even-even nuclei, Phys. Rev. **98**, 212 (1955).
[10] A. Bohr and B. R. Mottelson, Collective and individual-particle aspects of nuclear structure, Mat. Fys. Medd. K. Dan. Vidensk. Selsk. **27**, 16 (1953).
[11] S. F. Shen, Y. B. Chen, F. R. Xu, S. J. Zheng, B. Tang, and T. D. Wen, Signature for rotational to vibrational evolution along the yrast line, Phys. Rev. C **75**, 047304 (2007).
[12] Q. Yang, H. L. Wang, M. L. Liu, and F. R. Xu, Characteristics of collectivity along the yrast line in even-even tungsten isotopes, Phys. Rev. C **94**, 024310 (2016).
[13] H. Y. Meng, Y. W. Hao, H. L. Wang, and M. L. Liu, Signature of yrast-state structure in even-even hafnium isotopes based on traditional total-Routhian-surface calculations and novel E-GOS curves, Prog. Theor. Exp. Phys. **2018**, 103D02 (2018).
[14] J. Yang, H. L. Wang, Q. Z. Chai, M. L. Liu, and F. R. Xu, Evolution of shape and rotational structure in neutron-deficient 118C128Ba nuclei, Prog. Theor. Exp. Phys. **2016**, 063D03 (2016).
[15] H. F. Li, H. L. Wang, and M. L. Liu, Nuclear collectivity in the even-even $^{164-178}$Yb along the yrast line, Nucl. Sci. Technol. **30**, 14 (2019).
[16] R. Bengtsson, S. Frauendorf, and F. R. May, Quasiparticle levels in rotating rare earth nuclei: A cranked shell-model dictionary, At. Data Nucl. Data Tables **35**, 15 (1986).
[17] W. Nazrewicz, R. Wyss, and A. Johnson, Structure of superdeformed bands in the $A \approx 150$ mass region, Nucl. Phys. A **503**, 285 (1989).
[18] W. Satuła, R. Wyss, and P. Magierski, The Lipkin-Nogami formalism for the cranked mean field, Nucl. Phys. A **578**, 45 (1994).
[19] F. R. Xu, P. M. Walker, and R. Wyss, Limit to high-spin isomerism in hafnium isotope, Phys. Rev. C **62**, 014301 (2000).
[20] P. Möller, J. R. Nix, W. D. Myers, and W. J. Swiatecki, Nuclear ground-state masses and deformations, At. Data Nucl. Data Tables **59**, 185 (1995).
[21] T. R. Werner and J. Dudek, Shape coexistence effects of super- and hyperdeformed configurations in rotating nuclei with $58 \leqslant Z \leqslant 74$, At. Data Nucl. Data Tables **50**, 179 (1992).

[22] D. R. Inglis, Particle derivation of nuclear rotation properties associated with a surface wave, Phys. Rev. **96**, 1059 (1954).
[23] D. R. Inglis, Dynamics of nuclear deformation, Phys. Rev. **97**, 701 (1955).
[24] D. R. Inglis, Nuclear moments of inertia due to nucleon motion in a rotating well, Phys. Rev. **103**, 1786 (1956).
[25] J. Dudek, B. Herskind, W. Nazarewicz, Z. Szymanski, and T. R. Werner, Pairing, temperature, and deformed-shell effects on the properties of superdeformed ^{152}Dy nucleus, Phys. Rev. C **38**, 940 (1988).
[26] W. Nazarewicz, J. Dudek, R. Bengtsson, T. Bengtsson, and I. Ragnarsson, Microscopic study of the high-spin behaviour in selected $A \approx 80$ nuclei, Nucl. Phys. A **435**, 397 (1985).
[27] V. M. Strutinsky, Shell effects in nuclear masses and deformation energies, Nucl. Phys. A **95**, 420 (1967).
[28] H. C. Pradhan, Y. Nogami, and J. Law, Study of approximants in the nuclear pairing-force problem, Nucl. Phys. A **201**, 357 (1973).
[29] W. Satuła and R. Wyss, Extended mean field description of deformed states in neutron deficient Cd- and Sn-nuclei, Phys. Scr. T **56**, 159 (1995).
[30] P. Möller and J. R. Nix, Nuclear pairing models, Nucl. Phys. A **536**, 20 (1992).
[31] H. Sakamoto and T. Kishimoto, Origin of the multipole pairing interactions, Phys. Lett. B **245**, 321 (1990).
[32] F. R. Xu, W. Satuła, and R. Wyss, Quadrupole pairing interaction and signature inversion, Nucl. Phys. A **669**, 119 (2000).
[33] W. Satula and R. Wyss, Mean-field description of high-spin states, Rep. Prog. Phys. **68**, 131 (2005).
[34] P. Ring, R. Beck, and H. J. Mang, On the application of the Hartree-Fock-Bogolyubov-equations to a microscopic theory of nuclear rotations, Z. Phys. **231**, 10 (1970).
[35] W. D. Myers and W. J. Swiatecki, Nuclear masses and deformations, Nucl. Phys. **81**, 1 (1966).
[36] S. Cwiok, J. Dudek, W. Nazarewicz, J. Skalski, and T. Werner, Single-particle energies, wave functions, quadrupole moments and g-factors in an axially deformed Woods-Saxon potential with applications to the two-centre-type nuclear problems, Comput. Phys. Commun. **46**, 379 (1987).
[37] A. Bhagwat, X. Vinas, M. Centelles, P. Schuck, and R. Wyss, Microscopic-macroscopic approach for binding energies with the Wigner-Kirkwood method, Phys. Rev. C **81**, 044321 (2010).
[38] S. Raman, C. W. Nestor, and P. Tikkanen, Transition probability from the ground to the first-excited 2^+ state of even-even nuclides, At. Data Nucl. Data Tables **78**, 1 (2001).
[39] N. J. Stone, Table of nuclear magnetic dipole and electric quadrupole moments, At. Data Nucl. Data Tables **90**, 75 (2005).
[40] N. Fouladi, J. Fouladi, and H. Sabri, Investigation of low-lying energy spectra for deformed prolate nuclei via partial dynamical $SU(3)$ symmetry, Eur. Phys. J. Plus **130**, 112 (2015).
[41] R. F. Casten, D. S. Brenner, and P. E. Haustein, Valence *pn* Interactions and the Development of Collectivity in Heavy Nuclei, Phys. Rev. Lett. **58**, 658 (1987).
[42] R. F. Casten, Possible Unified Interpretation of Heavy Nuclei, Phys. Rev. Lett. **54**, 1991 (1985).
[43] R. F. Casten, N_pN_n systematics in heavy nuclei, Nucl. Phys. A **443**, 1 (1985).
[44] R. F. Casten and N. V. Zamfir, The evolution of nuclear structure: The N_pN_n scheme and related correlations, J. Phys. G: Nucl. Part. Phys. **22**, 1521 (1996).
[45] J. Dudek, W. Nazarewicz, and P. Olanders, On the shape consistency in the deformed shell-model approach, Nucl. Phys. A **420**, 285 (1984).